Available online at www.sciencedirect.com
ScienceDirect
Marine Chemistry 106 (2007) 239–255
MARINE CHEMISTRY
www.elsevier.com/locate/marchem

A non-steady state diagenetic model for changes in sediment biogeochemistry in response to seasonally hypoxic/anoxic conditions in the "dead zone" of the Louisiana shelf

John W. Morse [a,*], Peter M. Eldridge [b]

[a] Department of Oceanography, Texas A and M University, College Station, TX 7784-3136, United States
[b] U.S. Environmental Protection Agency–Coastal Ecology Branch, WED/CEB, 2111 S.E. Marine Science Drive, Newport, OR 97365, United States

Received 2 August 2005; received in revised form 31 January 2006; accepted 17 February 2006
Available online 6 March 2006

Abstract

Biogeochemical processes occurring near the sediment–water interface can play an important role in the establishment and persistence of hypoxic-to-anoxic conditions in areas of moderate-to-shallow water depth. Results are given in this paper for diagenetic modeling of two sites from the area on the Louisiana shelf west of the Mississippi River Delta known as the "dead zone". This is one of the largest and most studied regions where seasonal coastal hypoxia occurs. The diagenetic model was capable of generating good matches with depth profiles at both sites in the upper 8 cm. Moderate differences between predicted and observed concentrations below this depth are most likely due to the highly non-steady state conditions in this region. The model was also able to predict extremely low dissolved sulfide concentrations and bacterial sulfate reduction rates that were in good agreement with independent direct observations. A sensitivity analysis of the model to input parameters showed that the model was much more sensitive to changes in values under hypoxic conditions than norm-oxic or anoxic conditions in the overlying water.

Simulations were carried out to first determine how the profiles of sediment porewater parameters and interfacial fluxes would change under differing quasi-steady state conditions where overlying dissolved oxygen concentrations and the rate of bioirrigation were varied. Next a non-steady state simulation was run to investigate how sediment biogeochemistry would change between these conditions during a hypothetical annual cycle. Results demonstrated a clear need to better understand the dynamic relationship among overlying water oxygen concentrations, the behavior of the benthic faunal community responsible for bioirrigation and sediment biogeochemistry.

Keywords: Diagenetic model; Hypoxia; Louisiana shelf

1. Introduction

Although the bottom waters of many freshwater and marine environments are either permanently oxic or anoxic, there is a growing appreciation that in many bodies of water near-bottom conditions may seasonally oscillate between these extremes (e.g., Chesapeake Bay, Sannich Inlet, Offatts Bayou and Corpus Christi Bay, Texas, and the Louisiana shelf west of the Mississippi River). Interest has been growing (e.g., Malakof, 1998) in regard to the potential exacerbation of seasonal hypoxic/anoxic conditions in estuarine and near coastal areas by

* Corresponding author. Tel.: +1 979 845 9630; fax: +1 845 9631.
E-mail address: Morse@ocean.tamu.edu (J.W. Morse).

0304-4203/$ - see front matter © 2006 Elsevier B.V. All rights reserved.
doi:10.1016/j.marchem.2006.02.003

anthropogenic impacts associated with increased nutrient input (e.g., see special issue of Estuaries, 1994; Zimmerman and Canuel, 2000). Although observational databases for these environments have increased greatly over roughly the last decade, a quantitative understanding of the dynamics of their physical, chemical and ecological systems is not well established.

For estuarine and coastal waters of relatively shallow to moderate depth, benthic processes, involving the transport of oxidized and reduced species across the sediment–water interface, can play an important role in influencing the redox conditions of overlying waters (Jørgensen et al., 1990; Roden and Tuttle, 1992; Cooper and Morse, 1996; Sell and Morse, 2006). For example, a high benthic oxygen demand (BOD) associated with the heterotrophic oxidation of sedimentary organic matter can lead to anoxic conditions in the overlying water. This in turn can lead to the death or flight of benthic macro and meio faunal organisms responsible for bioturbation and bioirrigation (e.g., Blackwelder et al., 1996; Gupta et al., 1996). As a result oxidative reactions and transport of solid and dissolved species can be greatly slowed. Under such conditions sedimentary sulfides can build up and dissolution of carbonate minerals may slow or stop. When oxic conditions return to the overlying water there can be a major "oxygen debt" of reduced species accumulated near the sediment–water interface that may buffer the reestablishment of early oxic conditions. It is clear that, in areas where seasonal hypoxia/anoxia occurs, major non-steady state conditions exist not only in the water column, but also in the underlying sediments (e.g., Kristiansen et al., 2002).

We have used our earlier field studies on the Louisiana shelf west of the Mississippi River (Lin and Morse, 1991; Morse and Berner, 1995; Rowe et al., 1995, 2002; Morse and Rowe, 1999; Morse unpublished data) to construct a diagenetic model for the response of sediment biogeochemistry to seasonal changes in the redox conditions of the overlying waters (e.g., Rabalais et al., 1994, 2002). Our basic approach was to apply the diagenetic model of Eldridge and Morse (2000), that is largely derived from the earlier diagenetic models of Van Cappellen and Wang (1996) and Boudreau (1996), to sediments in the study area. The model was modified appropriately for the sediments on the Louisiana shelf and non-steady state redox conditions of the overlying waters. The model was first developed and tested on existing sediment biogeochemical profiles. Model outputs were compared with independent measurements of bacterial sulfate reduction rates. Next, testing was done via sensitivity analysis of input parameters to identify which of the parameters the model outputs were most responsive to under different overlying water oxygen concentrations. These results were then used as "guide posts" in constructing the time dependent model.

Although there are significant uncertainties in the results of our the modeling efforts, they do set some interesting bounds and point the way to what types of new data and sampling strategies will be required to further refine our understanding of these complex and important systems.

2. Background observational information

Hypoxic, defined as <2 mg L^{-1} dissolved oxygen (DO), to anoxic (including sulfidic) conditions are common on the Louisiana shelf along the coast west of the Mississippi River Delta in the summer. These conditions primarily occur in the period from about mid-June to mid-August. The intensity and extent of these hypoxic/anoxic events are influenced by the interplay of many factors. Hypoxic to anoxic conditions can range from days to months in their duration (see Rabalais et al., 1994, 2002). From the modeling standpoint, this means no simple pattern for changes in water DO content can be used and its variability can be very stochastic during the summer. However, it does point to the need for a model that can be used to examine the potential impacts of different time periods of low-to-no DO in the overlying waters.

Our modeling effort will utilize data from two sites studied by Morse and Rowe (1999) in the Mississippi bight at about 20 m depth (sites 2b and 3). Although relatively close together (see Fig. 1, Morse and Rowe, 1999), Site 2b (29°07.1′N, 89°44.4′W) was overlain by moderately hypoxic (1.1 mg L^{-1} or 34 μM DO) waters, whereas Site 3 (29°06.5′N, 89°35.7′W) had close to

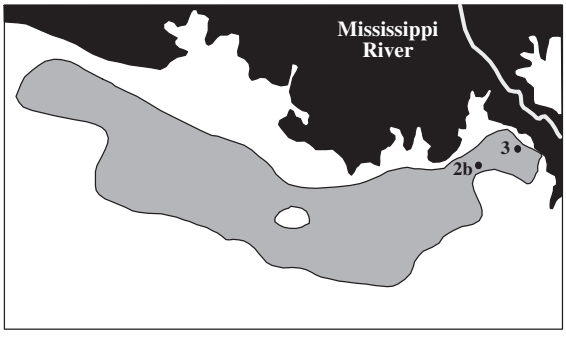

Fig. 1. The Mississippi Plume off the Louisiana coast was the site for the development work on the sediment diagenetic model. The location map shows the position of the data collection sites used for the model calibration. The grey region is the seasonally hypoxic "dead zone".

Table 1
Data from sites 2b and 3 used in model

Depth (cm)	Porosity		<63 μm (%)		$CaCO_3$ (wt.%)		Org-C (wt.%)		TRS (μmol/g)		AVS (μmol/g)	
	2b	3	2b	3	2b	3	2b	3	2b	3	2b	3
0–1	0.79	0.73	87	49	5.0	3.2	0.82	0.51	158	88	2.8	2.3
1–2	0.77	0.62	87	45	3.8	3.1	0.76	0.44	136	100	2.7	1.0
2–4	0.71	0.60	90	55	3.3	4.8	0.55	0.44	82	94	0.2	0.4
4–6	0.72	0.57	96	60	2.9	4.1	0.55	0.44	80	95	0.0	0.2
8–10	0.73	0.56	99	74	3.3	3.5	0.54	0.51	69	144	0.0	0.2
12–14	0.75	0.57	99	78	2.8	4.9	0.53	0.52	79	182	0.0	0.2
16–18	0.74	0.59	99	78	2.9	3.2	0.49	0.51	83	169	0.2	0.2

Depth (cm)	SO_4^{2-} (mM)		Cl^- (mM)		NH_4^+ (μM)		Fe^{2+} (μM)		Mn^{2+} (μM)		pH		DIC (mM)	
	2b	3	2b	3	2b	3	2b	3	2b	3	2b	3	2b	3
0–1	32	28	637	533	229	166	43	50	57	60	7.43	7.19	2.80	2.73
1–2	26	30	516	604	202	205	48	77	63	47	7.14	7.00	3.00	2.70
2–4	26	30	505	612	242	262	66	45	52	43	7.12	7.01	3.26	3.02
4–6	27	30	490	623	226	269	48	87	34	33	7.10	7.02	3.26	3.08
8–10	25	31	501	617	207	219	85	82	30	39	7.19	7.09	3.29	3.30
12–14	26	31	531	632	242	215	57	105	30	39	7.25	7.13	3.37	3.24
16–18	26	31	481	627	291	242	62	87	28	23	7.24	7.04	3.10	2.97

Site	*t* (°C)	S
2b	27.2	32.1
3	28.7	27.9

Depth (cm)	SO_4^{2-} reduction rate (mmol m^{-3} d^{-1})	
	2b	3
0–5	79	62
5–10	29	60
10–15	18	18

anoxic (~ 0.04 mg L^{-1} or ~ 1.3 μM DO) overlying water and was near the delta. The data available for these sites are extensive. It includes extensive measurements of porewater and solid sediment chemistry, and radiotracer sulfate reduction rates (SRR). Additional data from nearby sites will also be used to augment these data (e.g., sediment accumulation rates and chlorophyll reactivity from Chen et al., 2005). The data used in our model are presented in Table 1. Porewater profiles for important dissolved components such as dissolved inorganic carbon (DIC), NH_4^+, Fe^{2+}, and Mn^{2+} were similar at the two sites (Table 2; Fig. 2). Although sulfate reduction was an active process at both sites (14 and 16 mmol m^{-2} d^{-1} at sites 2b and 3 respectively), resulting in the accumulation of substantial concentrations of total reduced inorganic sulfur (TRS), dissolved sulfide was not detectable (<10 μM) in porewaters. This was likely the result of the high dissolved Fe^{2+} concentrations in the porewaters that limited dissolved sulfide via iron sulfide mineral formation.

Major differences in fluxes appear to be primarily the result of the lack of oxic respiration at Site 3 due to the close to anoxic conditions in the overlying water. At Site 2b the flux of oxygen into the sediment was close to the same as the flux of carbon dioxide out of the sediment. Therefore, even though sulfate reduction was the dominant heterotrophic process in the sediments at Site 2b, the almost complete oxidation of the produced sulfide must occur (i.e., here BOD is a good estimate of total benthic heterotrophic activity). Additionally, Site 3 had coarser grained sediment, less organic matter (OM) that also was of lower reactivity, and lower porosities than Site 2b. The coarser-grained nature of the sediment and the lower reactivity of the labile OM are possibly due to Site 3 being closer to the delta coast and receiving a greater proportion of coarse-grained sediment containing more terrestrial OM.

Morse and Rowe (1999) established many of the general relationships among the various parameters and environmental conditions that served as a conceptual

Table 2
Comparison of average values of parameters used in model as the ratio Site 3 to Site 2b

Parameter	Ratio 3/2b
Porosity	0.81
<63 μm	0.67
$CaCO_3$	1.11
Org-C	0.79
TRS	1.27
AVS	0.78
SO_4^{2-}	1.13
Cl^-	1.16
NH_4^+	0.96
Fe^{2+}	1.31
Mn^{2+}	0.96
pH	0.98
DIC	0.95

Values where important disagreement occurs are in grey. Note general excellent agreement for porewater components and poor agreement for fluxes and sedimentation rates.

base for our modeling efforts. Our goal was to make certain that we could reasonably well model the direct observational data at these sites before embarking on the considerably more speculative investigation of the impacts of changing overlying water redox conditions on sediment biogeochemistry. An important caveat was that, lacking data to the contrary, we necessarily had to assume the response of the highly reactive components was sufficiently fast so that their observed distributions represented quasi-steady state conditions. As will be discussed later, this seems to have been a reasonable assumption near the sediment–water interface, but not so for deeper in the sediment where the response time to changes in overlying water chemistry would be expected to be longer.

3. The diagenetic model

The diagenetic model was largely derived from the model of Van Cappellen and Wang (1996) as described in Eldridge and Morse (2000). In this study, we further modified the model by adding equations for manganese, an element that was in low concentrations and could be ignored in the previous study. As in the earlier model, pH profiles were collected in the field and were imposed on model calculations of FeS saturation and other pH sensitive parameters. The new model calculates porewater fluxes. We broke out the fluxes due to Fickian diffusion processes from those due to non-local exchange due to irrigation processes. As in most aspects of the diagenetic model the formulation for irrigation is

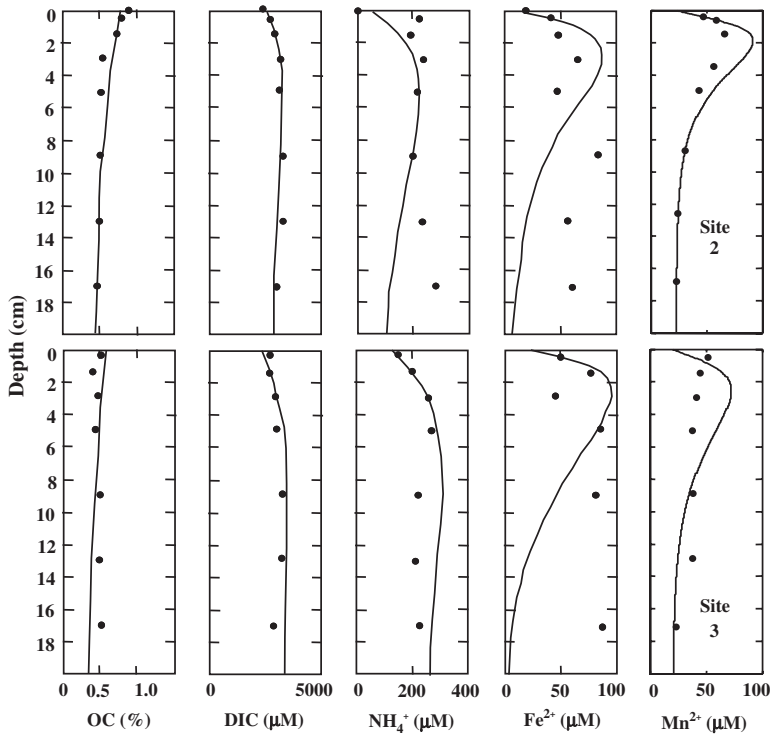

Fig. 2. Concentrations of dissolved components as with ● for data and line for model. Based on data of Morse and Rowe (1999).

only an approximation of a complex set of processes and its effectiveness diminishes as sediment conditions diverge from the model assumptions. For convenience we use a single irrigation coefficient (α_0) instead of multiple α_0, one for each geochemical porewater species. The single α_0 is slightly less accurate than multiple α_0 (Grigg et al., 2005). Of greater concern is that the accuracy of the non-local exchange formulation can be compromised when "substantial production or consumption occurs in a narrow band near a burrow wall" (Grigg et al., 2005). We found no information to suggest that our sites on the Gulf Shelf were different than other sites where non-local exchange formulations have been used. The non-local exchange model however may be

Table 3
This table shows the diagenetic reactions simulated in the model

Organic matter oxidations:

1. $(CH_2O)_x(NH_3)_y(H_3PO_4)_z + (x+2y)O_2 + (y+2z)HCO_3^- \xrightarrow{R_1/x} (x+y+2z)CO_2 + yNO_3^- + zHPO_4^{2-} + (x+2y+2z)H_2O$

2. $(CH_2O)_x(NH_3)_y(H_3PO_4)_z + \left(\frac{4x+3y}{5}\right)NO_3^- + \xrightarrow{R_2/x} \left(\frac{2x+4y}{5}\right)N_2 + \left(\frac{x-3y+10z}{5}\right)CO_2 + \left(\frac{4x+3y-10z}{5}\right)HCO_3^- + zHPO_4^{2-} + \left(\frac{3x+6y+10z}{5}\right)H_2O$

3. $(CH_2O)_x(NH_3)_y(H_3PO_4)_z + 2xMnO_2 + (3x+y-2z)CO_2 + (x+y-2z)H_2O \xrightarrow{R_3/x} 2xMn^{2+} + (4x+y-2z)HCO_3^- + yNH_4^+ + zHPO_4^{2-}$

4. $(CH_2O)_x(NH_3)_y(H_3PO_4)_z + 4xFe(OH)_3 + (7x+y-2x)HCO_3^- \xrightarrow{R_{41}/x} 4xFe^{2+} + (8x+y-2z)HCO_3^- + yNH_4^+ + zHPO_4^{2-} + (3x-y+2z)H_2O$

5. $(CH_2O)_x(NH_3)_y(H_3PO_4)_z + \left(\frac{x}{2}\right)SO_4^{2-} + (y-2z)CO_2 + (y-2z)H_2O \xrightarrow{R_5/x} \frac{x}{2}H_2S + (x+y-2z)HCO_3^- + yNH_3^+ + zHPO_4^{2-}$

Redox cycles:

8. $Fe^{2+} + \frac{1}{4}O_2 + 2HCO_3^- + \frac{1}{2}H_2O \xrightarrow{R_8} Fe(OH)_3 + 2CO_2$

10. $2Fe^{2+} + MnO_2 + 2HCO_3^- + 2H_2O \xrightarrow{R_{10}} Fe(OH)_3 + Mn^{2+} + 2CO_2$

11. $NH_4^+ + 2O_2 + 2HCO_3^- \xrightarrow{R_{11}} NO_3^- + 2CO_2 + 2H_2O$

12. $H_2S + 2O_2 + 2HCO_3^- \xrightarrow{R_{12}} SO_4^{2-} + 2CO_2 + 2H_2O$

14. $H_2S + 4CO_2 + 2Fe(OH)_3 \xrightarrow{R_{14}} 2Fe^{2+} + S^0 + 4HCO_3^- + 2H_2O$

15. $FeS + 2O_2 \xrightarrow{R_{15}} Fe^{2+} + SO4^{2-}$

23. $Fe^{2+} + 2HCO_3^- + H_2S \xrightleftharpoons{R_{23},R_{-23}} FeS + 2CO_2 + 2H_2O$

Alkalinity:

24. $CO_3^{2-} + \delta CO_2 + (1-\delta)H_2S \Longleftrightarrow (1-\delta)HCO_3^- + (1-\delta)HS^- + H_2O \qquad 0 \le \delta \le 1$

Eqs. (1)–(4) are replicated for refractory and labile organic matter. x, y, z are the component of oxidation contributed by CH_2O, NH_3, and H_3PO_4 respectively. Because we did not include all reactions from Van Cappellen and Wang (1996) the numbers in the table are not sequential, but refer to the numbering scheme used by these authors.

Table 4
Rate equations used in the reaction scheme (revised from Van Cappellen and Wang, 1996)

$R_1 = k_g\, rO_2$	$R_{11} = k_{11}[NH_4^+][O_2]$
$R_2 = k_g\, rNO_3^-$	$R_{12} = k_{12}TS[O_2]$
$R_3 = k_g\, rMn(IV)$	$R_{13} = k_{13}TS[MnO_2]$
$R_4 = k_g\, rFe(III)$	$R_{14} = k_{14}TS[Fe(OH)_3]$
$R_5 = k_g\, rSO_4^{2-}$	$R_{15} = k_{15}[FeS][O_2]$
$R_8 = k_8[Fe^{2+}][O_2]$	$R_{23} = K_{23}\sigma_{23}(\Omega_{FeS} - 1)$
$R_{10} = k_{10}[MnO_2][Fe^{2+}]$	$R_{-23} = K_{-23}\sigma_{-23}[FeS](1 - \Omega_{FeS})$
where:	
$\Omega_{FeS} = \frac{[Fe^{2+}][HS^-]}{\frac{[H^+]}{[H^+]+K_{H^+}} K'_{FeS}}$	$\Omega_{FeS} > 1$: $\delta_{23} = 1$, $\delta_{-23} = 0$
	$\Omega_{FeS} \leq 1$: $\delta_{23} = 0$, $\delta_{-23} = 1$

TS = $[H_2S] + [HS^-]$. Indexes on equation are the same as used by Van Cappellen and Wang (1996). Subscripted numbers refer to corresponding indices in Van Cappellen and Wang (1996).

more appropriate than other competing formulations (cylinder model) when there are "rapid episodic advective fluxes between sediment and overlying water" (Grigg et al., 2005). As will subsequently be shown, disturbance is an important aspect of our simulations. The equations of state are the same as in Eldridge and Morse (2000), but are repeated here for the convenience of the reader in Tables 3 and 4. The model was tested and used in five different ways:

1) A model calibration was made for assumed steady state conditions at the two stations;
2) A comparison was conducted of model-predicted fluxes and sulfate reduction rates with observed values;
3) A sensitivity analysis was made to investigate how model input parameters affect simulated results;
4) Model runs were made for Site 2b to predict different steady state conditions in the sediment, for changes in the overlying water O_2 concentration and estimated associated changes in bioturbation and bioirrigation; and
5) The model was modified to produce time-dependent results for differing scenarios of non-steady state conditions in transition between the conditions in (4).

4. Steady state model results

4.1. Calibration of steady state models of data for different sites and comparison of results with independent observations

The primary objective of the runs using presumed steady state conditions was to determine how differences in bottom water O_2 concentration affect sediment geochemistry. Input parameter values are given in Table 5.

At both sites (slightly hypoxic; Site 2b and nearly anoxic; Site 3) there was only at most a few millimeters penetration of O_2 into the sediments. The model always showed low concentrations of porewater sulfides (~ 20 μM HS^- plus H_2S) that were close to the sulfide analytical detection limit. The model consistently provided good fits between measured and modeled porewater Mn^{2+}, but the modeled Fe^{2+} profiles below 8 cm were lower than the measured profiles and the porewater Fe^{2+} and Mn^{2+} profiles were similar at sites 2b and 3. Modeled and measured OM and DIC exhibited a similar difficulty.

At Site 2b, in order to meet the DIC constraints, the model required that the labile OM input be ~ 5 times the size of the non-labile OM input. The reactivity of the labile pool was 20 y^{-1} which is on the same order of magnitude as that of phytoplankton (~ 50 y^{-1}; Heip et al., 1995; Minoru et al., 2002). The sediment profile inflection point of the DIC and reduced porewater metals occurred around 2 cm, suggesting that much of the OM mineralization took place within this surface 2 cm layer (Fig. 2). The dominance of OM mineralization near the sediment–water interface and the relative lack of a transport mechanism to mix the porewater NH_4^+ downward resulted in a general decease in NH_4^+ with depth, similar to that found in other poorly irrigated sediments (D'Andrea et al., 1996). Because the oxygen penetration depth was small, sulfate reduction was the dominate process below the first few millimeters. At Site 2b, the model predicted a SRR of 110 μM SO_4^{2-} d^{-1} at 0.75 cm below the sediment–water interface (Fig. 3). Although, there were no measurements above 3 cm into the profile, the decay of the measured SRR and the modeled SRR was the same at depth (Fig. 3).

The net DIC flux (Table 6) was −35 mmol C m^{-2} d^{-1}, which is close to that predicted from the integrated sulfate reduction rate of ~ 28 mmol C m^{-2} d^{-1}. The O_2 flux (Table 6) calculated from the model under hypoxic conditions is only 4.6 mmol C m^{-2} d^{-1}. When combined with the integrated sulfate reduction rate this reasonably matches the DIC flux. However, even if all the O_2 flux went to sulfide oxidation at least 80% of the produced sulfide would have to be buried or consumed via reaction with iron and manganese oxides.

In order to meet the [DIC] constraints at Site 3, the model required that the labile OM input be >3 times the size of the non-labile OM input, but the reactivity of the labile pool was only 7 y^{-1} which is about one third that used for Site 2b. There was no obvious inflection point in the measured or modeled DIC profile nor was there an obvious trend in porewater metals concentrations. The

Table 5
Values of input parameters used in calibration (2b, hypoxic and 3) and sensitivity analyses

Model parameter	Units	2b O_2 sat	2b hypoxic	2b anoxic	3 (Anoxic)
Surface biodiffusion (BD0)	$cm^2\ y^{-1}$		25		
Depth biodiffusion decrease	cm		18		
Depth biodiffusion goes to 0	cm		25		
OM rate constants	y^{-1}		20		7
OM rate constants	y^{-1}		0.080		
DOM rate constants	y^{-1}		35		20
Dissolution rate	y^{-1}		0.15		
K_{FeS}	$[mol\ L^{-1}]^2$		0.0006		
$k_8([Fe_2][O_2])$	$mol\ L^{-1}\ y^{-1}$		80		
$k_{10}([MnO_2][Fe^{2+}])$	$mol\ L^{-1}\ y^{-1}$		0.60		
$k_{11}([NH_4^+][O_2])$	$mol\ L^{-1}\ y^{-1}$		2.6		
$k_{12}([TS][O_2])$	$mol\ L^{-1}\ y^{-1}$		2600		
$k_{13}([TS][MnO_2])$	$mol\ L^{-1}\ y^{-1}$		0.10		
$k_{14}([TS][Fe(OH)_3])$	$mol\ L^{-1}\ y^{-1}$		10		
$k_{15}([FeS][O_2])$	$mol\ L^{-1}\ y^{-1}$		3		
$k_{23}([FeS]$	$mol\ g^{-1}\ y^{-1}$		10		
k_23([FeS])	$mol\ g^{-1}\ y^{-1}$		0.0028		
C:Ps atom L	None		105		
N:Ps atom L	None		25		20
P:Ps atom L	None		0.158		
C:Ps atom NL	None		105		
N:Ps atom NL	None		25		20
P:Ps atom NL	None		0.10		
C:Ps atom DOC	None		105		
N:Ps atom DOC	None		25		
P:Ps atom DOC	None		0.10		
kO_2	mM		0.040		
kNO_3^-	mM		0.025		
kMnO	mM		1400		
kFe(III)	mM		18,000		
kSO_4^{2-}	mM		800		
Irrigation coefficient	y		60	2.0	19
Advective velocity	$cm\ y^{-1}$		0.80	0.8	0.6
Benthic boundary O_2	mM	5000	34.4	2.0	2.0
Benthic boundary NO_3^{-1}	mM		25		
Benthic boundary NH_4^+	mM		50		120
Benthic boundary SO_4^{2-}	mM		26,000		
Benthic boundary TH_2S	mM		2.0		
Benthic boundary MnO_2	$mmol\ gdw^{-1}$		9300		5.0
Benthic boundary Mn^{2+}	mM		23		20
Benthic boundary R–Fe(III)	$mmol\ gdw^{-1}$		250,000		18,000
Benthic boundary Fe^{2+}	mM		1.0		
Benthic boundary FeS	$mmol\ gdw^{-1}$		250,000		100
Benthic boundary DOM	mM		20,000		
Benthic boundary TC	$mmol\ gdw^{-1}$		2400		2300
Benthic boundary DOMI	mM		16,000		17,000
Benthic boundary NH_4^+	mM		5.0		
OM1 flux	$mg\ C\ m^{-2}\ d^{-1}$	260	340		120
OM2 flux	$mg\ C\ m^{-2}\ d^{-1}$	120	70		30

If a data box is blank, the same value was used as for Site 2b (hypoxic).

lack of obvious gradients in this sediment resulted in a model calibration that required only 150 mg C m^{-2} d^{-1} for labile OM which is slightly less than half that predicted for Site 2b. The SRR was also about half that of Site 2b (Table 1, also see Fig. 3). A very low surficial flux of O_2 was a consequence of the very low bottom water O_2 concentrations and low labile OM flux. We used a low irrigation (19 cm^2 y^{-1}) coefficient for this site because there are few irrigating infauna under these low O_2 conditions (Rowe et al., 2002). The flux of O_2 was only about 10% of the DIC and most of the produced sulfide must be buried or react with metal oxides.

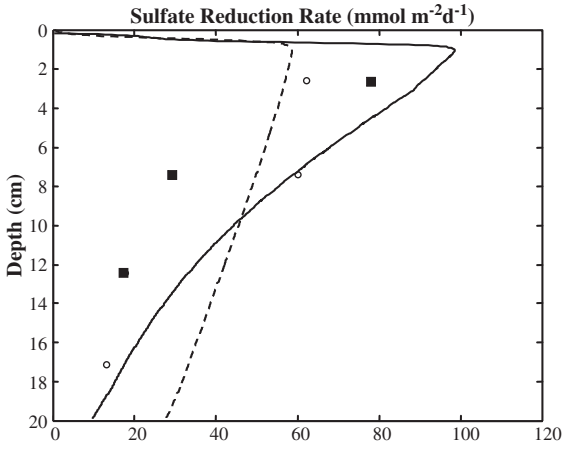

Fig. 3. Sulfate reduction measurements and model simulations for Site 2b (solid line and squares) and 3 (dashed Line and open circles). Lines are model generated and symbols are data from Morse and Rowe (1999).

In summary, the model is capable of generating good matches to depth profiles at both sites in the upper 8 cm. Moderate differences between predicted and observed concentrations below this depth are most likely due to the highly non-steady state conditions in this region. Further faith in model is gained from its ability to predict extremely low dissolved sulfide concentrations, and bacterial sulfate reduction rate depth profiles, that are in good agreement with independent direct observations for both sites, even though they differed in several important ways (e.g., overlying water DO, grain size and porosity, organic matter concentration and lability).

4.2. Sensitivity analyses

4.2.1. Method of analysis and general considerations

Examination of the sensitivity of the model outputs (here OM, DIC, NH_4^+, Fe^{2+}, and Mn^{2+} depth profiles) to input parameters provides a test of the model stability (Gold, 1977). Effects of input data (Table 5) variability were tested on the model by increasing and decreasing the value of each datum individually by 50% for most input parameters. The sensitivity of the models to these changes was determined by a measure of goodness of fit. This was done by using the root mean squared difference (RMSD) between the reference simulations for sites 2b and 3, and each altered simulation normalized by the reference site simulation mean (Table 5). It should be kept in mind that this approach primarily measures differences in the shape of the calculated concentration–depth profiles and does not involve qualities such as maximum or minimum concentrations, nor does it produce results such as comparison of integrated or mean values. The resulting RMSD values are consequently calculated as absolute (sign independent) fractions of the mean values.

Presentation of the results of the sensitivity tests is given in Table 7. They have been divided into four arbitrary categories based on the extent of influence. The first is comprised of input parameters that have a close to negligible influence (<0.1), the second is comprised of parameters that have a modest influence (0.10 to 0.99), the third is comprised of parameters that have major influence (1.00 to 4.99), and finally the fourth is comprised of those parameters that produce what are not likely to be "reasonable" results (>5). Table 7 does not include numeric data (as the large number of values is rather overwhelming), but rather the many data "boxes" have been shaded according to the defined range categories. In addition to results under observed conditions at sites 2b and 3, results are reported for simulations at Site 2b where overlying water was both saturated with dissolved oxygen and anoxic. Bioirrigation rates were kept constant for oxic and hypoxic conditions but set to very close to zero for anoxic conditions. Results are presented as four side-by-side shaded panels to provide for ease of comparison. Values of input parameters for the four sensitivity analyses are given in Table 5.

4.2.2. Results of sensitivity analyses

4.2.2.1. General results. In Table 7 it can be readily observed that model output is least sensitive to variation of the input parameter values under oxic conditions and most sensitive to changes in input parameter values under hypoxic conditions. Under anoxic conditions the impact of changing input parameters is generally slight-to-modest with close to a constant influence for a given output parameter. The differences between the modeled Site 2b Anoxic and Site 3 Observed are probably dominantly

Table 6
Fickian, irrigation (non-local exchange by irrigating infauna), and total surficial fluxes predicted by the model (mmol m^{-2} d^{-1})

Site	Fickian	Irrigation	Irrigation %	Net flux
2b				
O_2	4.1	0.56	12	4.6
DIC	−9.0	−25	73	−35
NH_4^+	−2.4	−7.9	76	−10
3				
O_2	0.15	0.02	12	0.17
DIC	−3.3	−12	79	−16
NH_4^+	−1.0	−4.1	79	−5.1

Positive numbers are fluxes into the sediments and negative fluxes are out of the sediment.

the result of the greater concentration of labile OM at Site 2b. This leads to OM not being sensitive at Site 2b, but slightly sensitive at Site 3, and the inverse being true for Mn^{2+} to changes in input parameters. These general observations are consistent with the model being more stable under strongly oxic or anoxic conditions, but less stable under the redox-transitional hypoxic conditions.

Table 7
Results of sensitivity analyses for most input parameters

Model parameter	2b Oxygen saturated										2b Hypoxic-observed									
	OM		DIC		NH_4^+		Fe^{2+}		Mn^{2+}		OM		DIC		NH_4^+		Fe^{2+}		Mn^{2+}	
	Max	Min	Max	Min	Max	Min	Max	Min	Max	Min	Max	Min	Max	Min	Max	Min	Max	Min	Max	Min
Surface biodiff. (BD0)																				
Depth biodiff. decrease																				
Depth biodiff. goes to 0																				
OM rate constants																				
OM rate constants																				
DOM rate constants																				
Dissolution rate																				
*K*FeS																				
$k8([Fe_2][O_2])$																				
$k10([MnO_2][Fe^{2+}])$																				
$k11([NH_4^+][O_2]$																				
$k12([TS][O_2])$																				
$k13([TS][MnO_2])$																				
$k14([TS][Fe(OH)_3])$																				
$k15([FeS][O_2])$																				
$k23([FeS]$																				
k_23 ([FeS])																				
C:Ps atom L																				
N:Ps atom L																				
P:Ps atom L																				
C:Ps atom NL																				
N:Ps atom NL																				
P:Ps atom NL																				
C:Ps atom DOC																				
N:Ps atom DOC																				
P:Ps atom DOC																				
kO_2																				
kNO_3^-																				
*k*Mn0																				
*k*Fe(III)																				
kSO_4^{2-}																				
Irrigation coefficient																				
Advective velocity																				
Benthic boundary O_2																				
Benthic boundary NO_3^{-1}																				
Benthic boundary NH_4^+																				
Benthic boundary SO_4^{2-}																				
Benthic boundary TH_2S																				
Benthic boundary MnO_2																				
Benthic boundary Mn^{2+}																				
Benthic boundary R–Fe(III)																				
Benthic boundary Fe^{2+}																				
Benthic boundary FeS																				
Benthic boundary DOM																				
Benthic boundary TC																				
Benthic boundary DOMI																				
Benthic boundary NH_4^+																				
OM1 flux																				
OM2 flux																				

(continued on next page)

Table 7 (*continued*)

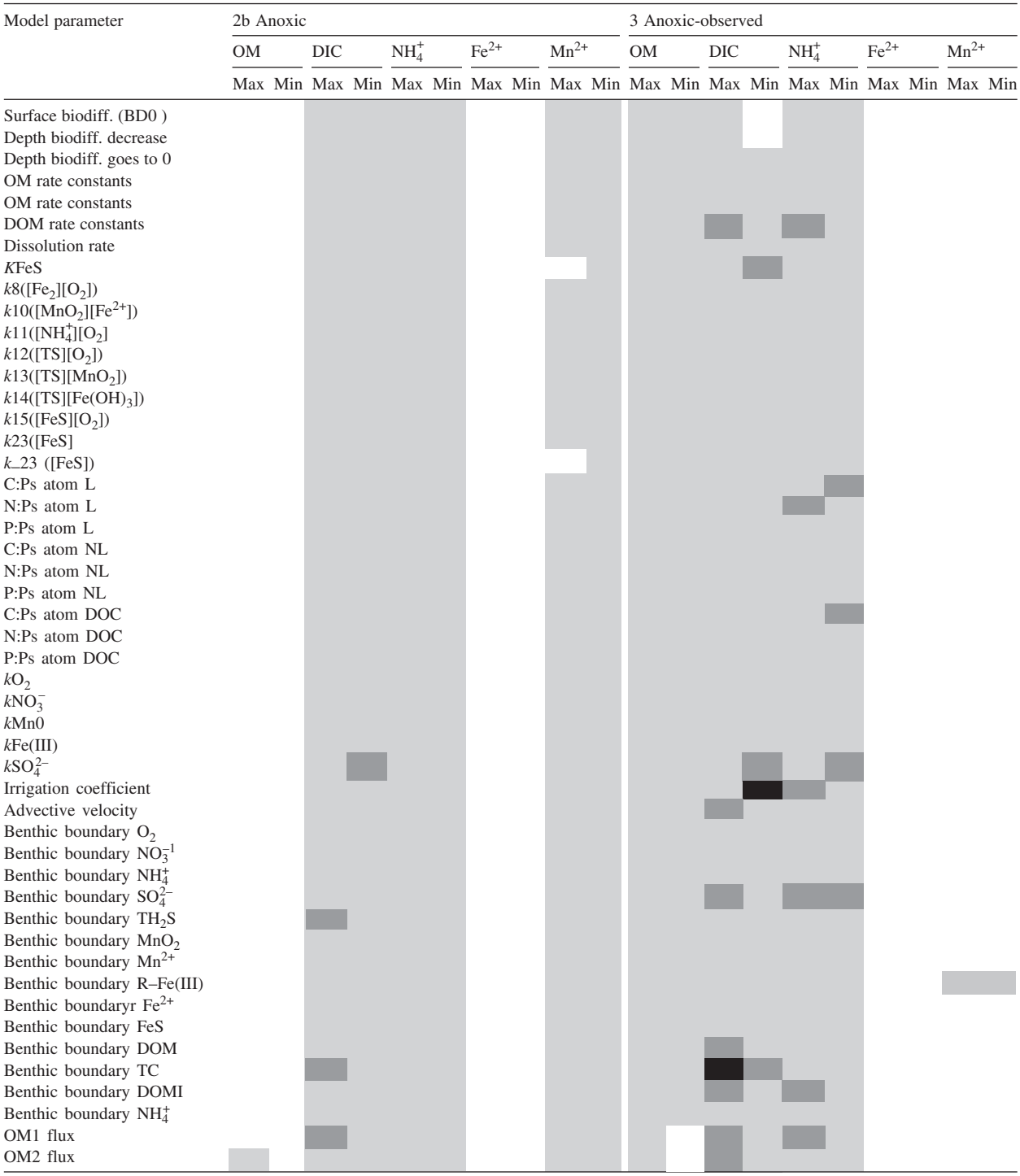

Max = 1.5 and Min = 0.5 times the model values used of input parameters. Shading in results boxes corresponds to the root mean squared difference (RMSD) values of blank = <0.10, light grey = 0.10 to 0.99, dark grey = 1.00 to 4.99 and black = ≥ 5.00. See text for further explanations.

Among the input parameters having the greatest sensitivity for both oxic and hypoxic conditions are those associated with macrofaunal activity (surface biodiffusion and the irrigation coefficient), the labile organic matter flux rate, benthic boundary DO concentration, sedimentation rate (advective velocity) and kSO_4^{2-}.

Macrofaunal activity and benthic boundary DO concentration are generally related and will be a focus of much of the following discussion of results of simulations of differing possible scenarios.

4.2.2.2. Sulfide. Dissolved sulfide concentrations are usually low to non-detectable near the sediment–water interface in Louisiana shelf sediments under oxic conditions as observed in this study and earlier work (e.g., Lin and Morse, 1991; Morse and Rowe, 1999), but dissolved sulfide has been observed in bottom waters under anoxic conditions (L. Cifuentes, personal communication). Our results are reasonably consistent with these observations in that the model predicts only low concentrations near the sediment–water but an increasingly strong build up of dissolved sulfide below about 10 cm with decreasing DO. Sulfide behavior will be discussed further in relation to possible scenarios later in this paper.

4.2.2.3. Dissolved oxygen flux. The DO flux (or benthic oxygen demand; BOD) is primarily controlled by three factors. The first is the concentration of DO in the benthic boundary water. Obviously when there is no DO in the overlying water the flux must be zero no matter how other parameters such the labile OM flux are varied. The DO flux becomes very sensitive to DO concentration under hypoxic conditions where, as a first order approximation, the flux becomes proportional to the concentration. However, it is also sensitive under both oxic and hypoxic conditions to the second major factor, the bioirrigation rate. The bioirrigation rate is also influenced by DO concentration, under hypoxic conditions, and, under oxic conditions, by the reestablishment of the benthic faunal communities. The third factor controlling DO flux can be the flux of labile OM. This is often likely to be the limiting factor under oxic conditions.

4.3. Steady state sediment biogeochemistry under differing conditions

Site 2b was chosen for a series of model runs under simulated steady state conditions to determine primarily the influences of differing DO concentrations in the overlying water and changes in sediment bioirrigation rates on the porewater chemistry of dissolved constituents and fluxes across the sediment–water interface. Site 2b was chosen because it is reasonably representative of sediments on the open Louisiana shelf in the seasonally hypoxic–anoxic "dead zone". The sensitivity tests also indicated that simulated anoxic conditions for Site 2b were very similar to those observed for Site 3, with the primary differences resulting from a greater concentration of labile organic matter at Site 2b.

The steady state simulations were made by setting the input parameters to given values indicative of natural Gulf Shelf conditions, hypoxia and anoxia. The model was run then for 50 years, which was more than adequate to produce steady state results. What these simulations do not address is the time and pathways necessary in natural systems to transit between the differing steady state environments. This issue will be addressed in the next subsection (Section 4.4).

Different conditions were used in a series of steady state model runs (Table 8) to simulate going from norm-oxic to anoxic and then back to norm-oxic conditions. Bioirrigation rates were adjusted to estimated appropriate values for each set of conditions. The return to oxic overlying water conditions was deemed to occur rapidly (e.g. a major storm mixes the water column), but return to original norm-oxic conditions was subdivided into initially no bioirrigation, moderate bioirrigation, from "pioneering" benthic fauna, and finally the original bioirrigation rate. Results are discussed for changes in OM, DIC, NH_4^+, Fe^{2+}, and Mn^{2+} depth profiles, dissolved sulfide depth profiles, and benthic DO fluxes.

The generally used sets of depth profiles for model results are shown in Fig. 4A for going from norm-oxic to anoxic conditions and in Fig. 4B for returning from anoxic to norm-oxic conditions. In going from oxic to anoxic conditions, OM exhibits an increase near the sediment–water interface. This is likely due to decreasing rates of OM oxidation. DIC and NH_4^+ show similar behavior with little change until anoxic conditions are

Table 8
Simulated sediment DO flux at different stages of recovery from an anoxic bottom water condition

Conditions	O_2 μM at sed. surface	Irrigation coefficient	Total O_2 flux	Fickian O_2 flux	Irrigation O_2 flux
Anoxia (no infauna)	2	2	0.26	0.26	0
Initial mixing (no infauna)	200	2	16	16	0.22
High O_2 (pioneering species)	200	10	17	16	1.1
Natural state (mature community)	200	100	27	15	11
Hypoxia (standard run)	34	30	4.6	4.1	0.56

Fluxes are in mmol O_2 m^{-2} d^{-1} and are separated into predicted interfacial Fickian and irrigating fluxes.

reached, at which point there is a significant build up in the concentrations of both constituents with increasing depth. This reflects the substantial decrease in transport rates under anoxic conditions where Fickian diffusion predominates. The primary influence on Fe^{2+} distribution is the major decrease in the depth at which its concentration approaches zero. This will subsequently be shown to be the result of dissolved sulfide build up resulting in FeS precipitation at shallower depths. Mn^{2+} has an increase in its shallow depth maximum in decreasingly oxic conditions and a large increase in its concentration at depth under anoxic conditions. This reflects its increasing importance as an electron acceptor and the change for bioirrigation-dominated to diffusion-dominated transport.

The model results for the return to norm-oxic conditions are the same for anoxic and norm-oxic conditions as in the previous example. The intermediate two cases where the overlying water is fully oxic but there are first no and then "pioneering" benthic organisms clearly illustrate the importance of the benthic community. These conditions generate intermediate profiles at depth for DIC and NH_4^+, and cause a deepening of the depth of zero concentration for Fe^{2+}. The oxic conditions, with no bioirrigation, left the Mn^{2+} profile little changed from anoxic conditions, whereas the moderate bioirrigation

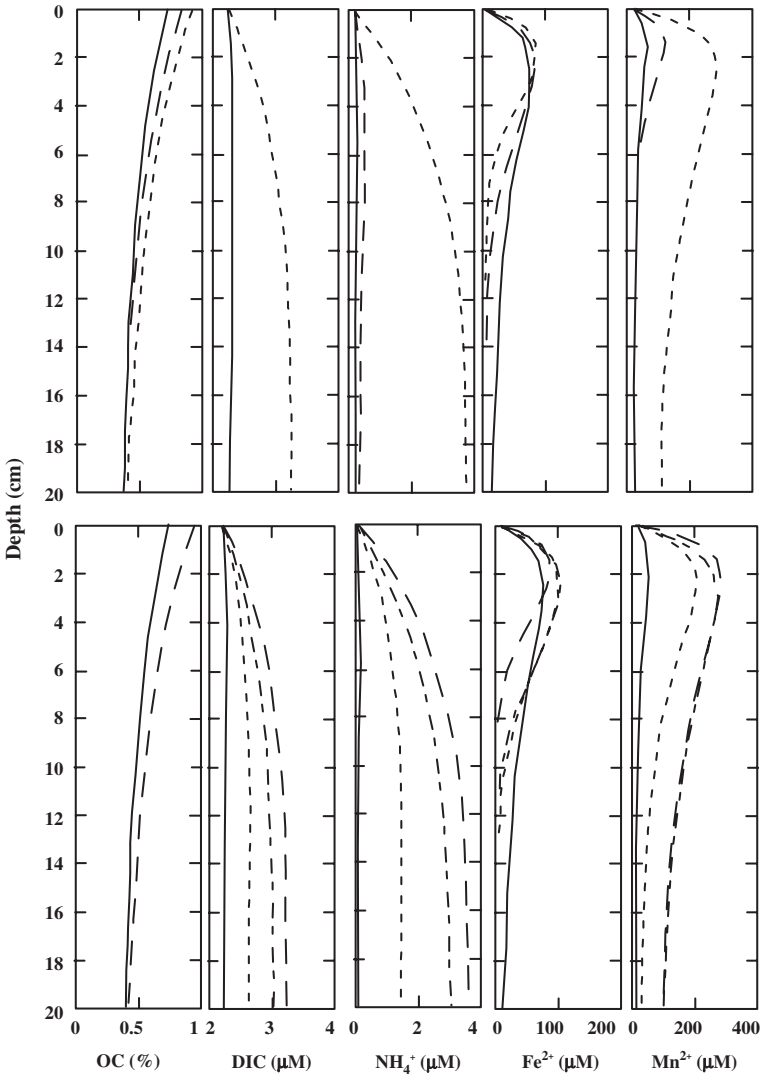

Fig. 4. Model depth profiles for variations in sediment concentrations of different components. The top set of plots is for going from oxic (solid) to hypoxic (long dash) to anoxic (short dash) overlying water conditions. The bottom set of plots is for going from anoxic (long dash), to oxic no bioirrigation (long and short dash), to oxic pioneering bioirrigation (short dash), to original oxic conditions (solid).

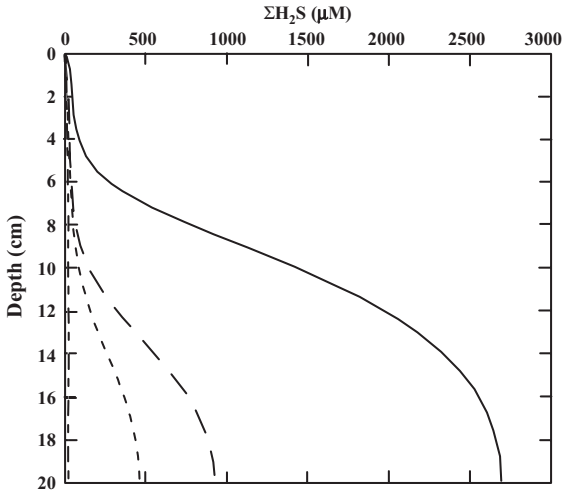

Fig. 5. Simulations of total dissolved sulfide concentration depth profiles under the differing conditions discussed in the text. Line types: solid = anaerobic; long dash = oxic no irrigation; short dash = oxic with pioneering species; long and short dash = natural state.

rate produced a profile intermediate between the norm-oxic and anoxic conditions.

Results for dissolved sulfide depth profiles are shown in Fig. 5. Under norm-oxic conditions with a fully developed benthic community, there is little change in dissolved sulfide concentration with depth and it always is at a low (few μM) concentration. Under anoxic conditions there is a rapid build up of dissolved sulfide below about 4 cm and it becomes close to constant below roughly 15 cm to close to 2.5 mM. The dissolved sulfide profiles for oxic conditions with no and moderate bioirrigation are intermediate between the previous two sulfide depth profiles. It is interesting that for oxic conditions, even with no bioirrigation, there is a substantial change in the dissolved sulfide depth profile compared to that found for anoxic conditions.

Among the most important parameters calculated in the model is the benthic DO flux (BOD). Results are given for the differing conditions in Table 8 as total, Fickian (diffusive) and irrigation DO fluxes. Total DO fluxes have also been plotted in Fig. 6 for the changing conditions as a time independent cycle. Under hypoxic conditions DO flux is only about 20% that found under norm-oxic conditions. However, under oxic no bioirrigation conditions, the DO flux is about 60% that under norm-oxic conditions and 3 times that under hypoxic conditions. These results clearly show the great sensitivity of benthic DO fluxes to both bottom water DO content and benthic faunal response to changing conditions (see also Archer and Devol, 1992). At full bioirrigation norm-oxic conditions, the BOD approaches the flux of DIC indicating most reduced electron acceptors are being oxidized instead of buried.

4.4. Time-dependent changes in sediment biogeochemistry with differing conditions

The objective of this simulation was to describe the onset of hypoxia, anoxia, and finally recovery of the sedimentary system in the Mississippi plume area. The simulation provides the same sequence of events shown in Fig. 4 using the steady state-conditions starting with well oxygenated bottom water and a mature benthic community (Condition 1) and the initial hypoxic model inputs from the Site 2B calibration (Condition 2). Bottom water O_2 concentrations were then reduced to 2 μM between weeks 10 and 30, (Condition 3). The recovery was simulated from week 30 to the end of the year the using the initial bottom O_2 concentration (200 μM).

As indicated by our sensitivity analysis, recovery from hypoxia/anoxia is strongly dependent on sediment irrigation by infauna. But little information is available concerning porewater O_2 concentrations and recruitment decisions of infauna (Marinelli and Woodin, 2002; Rowe et al., 2002) and relationship between infauna concentrations and irrigation (Marinelli, 1994; Martin and Banta, 1992). The pioneering studies by Marinelli and Woodin (2002) show that the behaviors of new recruits seem to follow changes in surficial oxygen concentrations and the steepness of oxygen gradients in the upper few mm of sediments. The organisms sense the lower oxygen concentrations associated with steeper O_2 gradients.

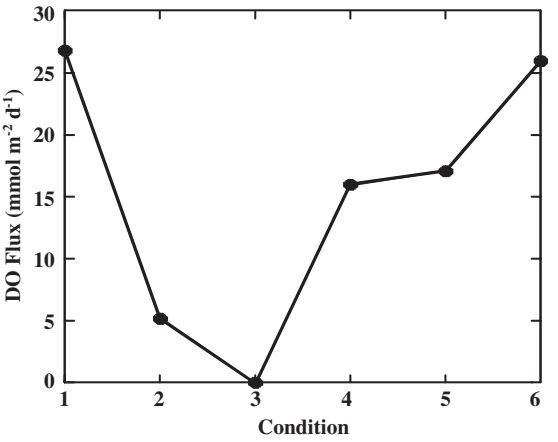

Fig. 6. Plot of DO fluxes under the various conditions modeled. Condition 1 = oxic with mature benthic community; Condition 2 = hypoxic; Condition 3 = anoxic; Condition 4 = oxic no bioirrigation; Condition 5 = oxic with pioneering level bioirrigation; Condition 6 = return to condition 1.

We developed an algorithm for the irrigation coefficient that was varied based on the O_2 concentration at 1 mm. Irrigation coefficients in this simulation were a function of the 1 mm O_2 concentration using a linear relationship that approximated the coefficients in steady state simulations (Table 8) ($\alpha_0 = 2.0 + 0.5[O_2]$) where α_0 is the irrigation coefficient and $[O_2]$ is the oxygen concentration at 1 mm.

Diaz and Rosenburg (1995) in their review of benthic infauna response to hypoxia show a number of case studies in which infauna respiration appeared not to be significantly affected until O_2 concentrations reached below 2 mL L^{-1}. This would seem to explain why our calibration of Site 3 required a relatively high irrigation coefficient and supports the relatively rapid increase in α_0 with O_2 at 1 mm.

The model provided output for each week over the span of a year. We examined the changes in 8 simulation output concentration variables that include solid and porewater constituents. Consistent with the sensitivity analysis, DIC concentration was most effected by the altered bottom water O_2 conditions and the porewater $[Mn^{2+}]$ and sulfide were affected to a lesser degree. The SOM, FeS, ferric iron, and manganese oxide minerals were unchanged (not shown). Dissolved Fe^{2+} changed by about 10 μM early in the simulation, but remained constant thereafter (Fig. 7).

When changes in concentration did occur, the model indicated that the maximum change happened within the first 5 cm. The exception to this was the sulfide concentrations that increased with depth throughout the simulation. While the effect of bottom water O_2 on DIC covered much of the 0–20 cm profile, changes in the porewater Fe^{2+} and Mn^{2+} profiles were restricted to 0–10 cm part of the profile during the transition from hypoxia to anoxia. During the recovery phase there was a

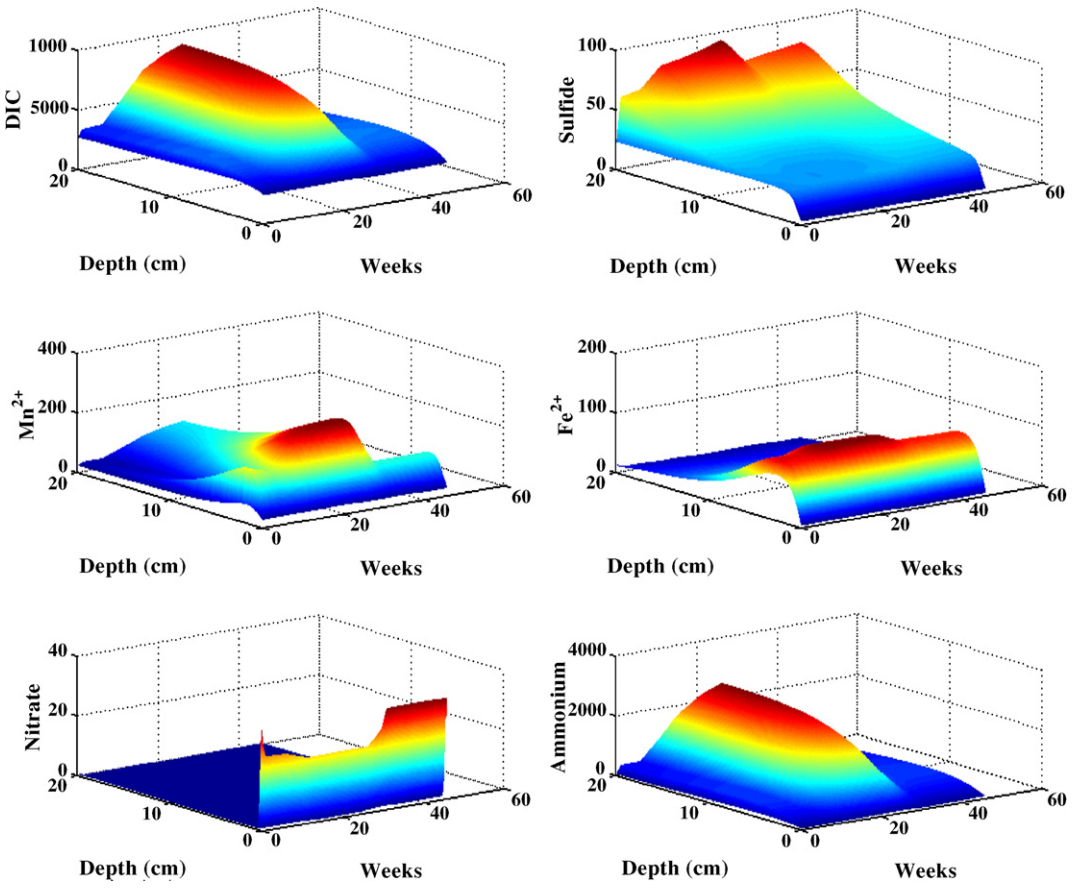

Fig. 7. Porewater DIC, sulfide, manganese, and iron concentrations in depth profile and over time. The simulations use the conditions from Fig. 6; starting with the initial conditions from oxic mature benthic community (Condition 1) but O_2 concentrations were reduced to those found at our hypoxic site (34 μM) (Condition 2), at weeks 10 through 30 the O_2 concentrations were again reduced to the conditions for the anoxic site (2 μM) (Condition 3). At week 30 bottom water O_2 concentrations were increased to 200 μM and the recovery conditions 4 through 6 were simulated in the time-series. Changes in coefficient of irrigation are described in the text and Table 1.

distinct shoaling of Fe^{2+} and Mn^{2+} concentration peaks towards the surface that intensified with increasing irrigation. This transition was accompanied by a pulse of electron donors from the sediment surface in the form of DIC and NH_4^+ (Fig. 8). The pulse was not symmetrical but instead could be characterized as a near square wave on the front end of the peak and then a relaxation to a steady state after several weeks. The square wave beginning of the pulse is due to the absence of a lag period for infaunal invasion of the sediments and population growth. The pulse of electron donors is probably realistic and represents the clearing of the reservoir of reduced metabolites built up during the anoxia.

Although there has been significant advances in quantifying irrigation (Meile et al., 2001) and the response of individual infaunal to hypoxia (Marinelli and Woodin, 2002; Diaz and Rosenburg, 1995), there is little information available about the rate of infaunal population growth or loss in response to either the onset of hypoxia and anoxia or the recovery of the benthos from these events. Influences of seasonal changes in temperature and particulate organic carbon input on a potentially changing population of benthos are also largely not quantified. In this regard, the observations of Rowe (personal communication, 2005) are relevant. Having worked extensively in this area, he has found that large fauna capable of major irrigation activity are largely absent year round, but that small bioturbators, such as nematode worms and polychaetes, are present year round regardless of the concentration of bottom water oxygen. Thus the system may stay close to our 'pioneering" condition at its maximum and quickly recover from low oxygen conditions. Clearly more complete chemical and biological studies on a seasonal basis are necessary to resolve these issues. However, the model presented in this paper provides a basis for designing and interpreting the results of such studies.

5. Conclusions

The diagenetic model presented in this paper was capable of being calibrated for steady state conditions at two stations; one hypoxic and the other close to anoxic, in the "dead zone" of the seasonally hypoxic–anoxic region of the Louisiana shelf west of the Mississippi River. However, the fit to model results was not as good below about 8 cm depth, probably due to the non-steady state conditions in the overlying water DO content. Sensitivity tests indicated that the model was substantially more sensitive to changes in the values of input parameters under hypoxic conditions than under normoxic or anoxic conditions. Simulations were carried out in which overlying water DO concentrations and bioirrigation rates were varied. These simulations demonstrated the importance of both of these factors in influencing the concentration and distribution of dissolved porewater components and interfacial flux rates. Although, during periods in which overlying DO is decreasing, these two parameters become linked as hypoxic conditions evolve, they are not directly linked if

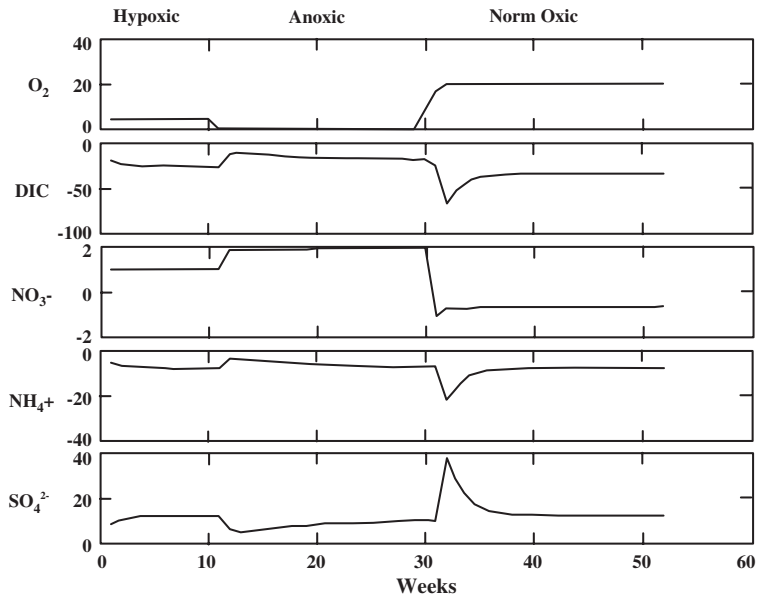

Fig. 8. Conditions for the time-series are as in Fig. 7, but results show flux of O_2, DIC, NO_3^-, NH_4^+, and SO_4^{2-} in mmol m^{-2} d^{-1}.

oxic conditions rapidly return as a result of mixing of the water column. Under these new oxic conditions, the rate of reestablishment of the benthic faunal community that is responsible for bioirrigation becomes important. The model points to the need for a better understanding of this process and its relationship to sediment biogeochemistry.

Acknowledgements

This paper is dedicated to Prof. Roland Wollast, who had a considerable influence on the career of JWM. They interacted while JWM was graduate student during the wonderful carbonate geochemistry field courses led by Fred Mackenzie at the Bermuda Biological Station for Research in the summers of 1970 and 1971. Later Prof. Wollast was the outside reader on JWM's PhD. dissertation and they remained in contact throughout the ensuing years with many shared interests in topics such as the behavior of magnesian calcites and early diagenesis. Support for this work was provided by the Louis and Elizabeth Scherck Endowed Chair in Oceanography (JWM). This document has been subject to EPA peer and administrative review, and has been approved for publication. Mention of trade names or commercial products does not constitute endorsement or recommendation for use. We thank Drs. Gilbert Rowe and Jack Middelburg who reviewed this paper. Their insightful comments lead to considerable improvements.

References

Archer, D., Devol, A., 1992. Benthic oxygen fluxes on the Washington shelf and slope: a comparison of in situ microelectrode and chamber flux measurements. Limnology and Oceanography 37, 614–629.

Blackwelder, P., Hood, T., Avarez-Zarikian, C., Nelson, T.A., McKee, B., 1996. Benthic Foraminifera from the NECOP study area impacted by the Mississippi River plume and seasonal hypoxia. Quaternary International 31, 19–36.

Cooper, D.C., Morse, J.W., 1996. The chemistry of Offatts Bayou, Texas: a seasonally highly sulfidic basin. Estuaries 19, 595–611.

Chen, N., Bianchi, T.S., McKee, B.A., 2005. Early diagenesis of chloropigment biomarkers in the lower Mississippi River and Louisiana shelf: implications for carbon cycling in a river-dominated margin. Marine Chemistry 93, 159–177.

Boudreau, B., 1996. A method-of-lines code for carbon and nutrient diagenesis in aquatic sediments. Computers & Geosciences 22, 479–496.

D'Andrea, A.F., Craig, N.I., Lopez, G.R., 1996. Benthic macrofauna and depth of bioturbation in Ecokernfoerde Bay. Geo-Marine Letters 16, 155–159.

Diaz, R.J., Rosenburg, R., 1995. Marine benthic hypoxia: a review of its ecological effects and the behavioral responses of benthic macrofauna. In: Ansell, A.D., Gibson, R.N., Barnes, M. (Eds.), Oceanography and Marine Biology an Annual Review, vol. 33, pp. 245–304.

Eldridge, P.M., Morse, J.W., 2000. A diagenetic model for sediment–seagrass interactions. Marine Chemistry 70, 89–104.

Estuaries, 1994. Special issue on NOAA's nutrient enhanced coastal ocean productivity study. Estuaries 17, 729–903.

Gold, H., 1977. Mathematical Modeling of Biological Systems: an Introductory Guidebook. Wiley-Interscience, New York.

Grigg, N.J., Boudreau, B.P., Webster, I.T., Ford, P.W., 2005. The non-local model of porewater irrigation: limits to its equivalence with a cylinder diffusion model. Journal of Marine Research 63, 437–455.

Gupta, B.K.S., Turner, R.E., Rabalais, N.N., 1996. Seasonal oxygen depletion in continental-shelf waters of Louisiana: historical record of benthic foraminifers. Geology 24, 227–230.

Heip, C.H.R., Goosen, N.K., Herman, P.M.J., Kromkamp, J., Middleburg, J.J., Soetaert, K., 1995. Production and consumption of biological particles in temperate tidal estuaries. Oceanography and Marine Biology, an Annual Review 33, 1–149.

Jørgensen, B.B., Bang, M., Blackburn, T.H., 1990. Anaerobic mineralization in marine sediments from the Baltic Sea–North Sea transition. Marine Ecology. Progress Series 59, 39–54.

Kristiansen, K.D., Kristensen, E., Jensen, M.H., 2002. The influence of water column hypoxia on the behavior of manganese and iron in sandy coastal marine sediment. Estuarine, Coastal and Shelf Science 55, 645–654.

Lin, S., Morse, J.W., 1991. Sulfate reduction and iron sulfide mineral formation in Gulf of Mexico anoxic sediments. American Journal of Science 291, 55–89.

Malakof, D., 1998. Death by suffocation in the Gulf of Mexico. Science 221, 190–192.

Marinelli, R.L., 1994. Effect of burrow ventilation on activities of a terebellid polychaete and silicate removal from sediment pore waters. Limnology and Oceanography 39, 303–317.

Marinelli, R.L., Woodin, S.A., 2002. Experimental evidence for linkages between infauna recruitment, disturbance, and sediment surface chemistry. Limnology and Oceanography 47, 221–229.

Martin, W.R., Banta, G.T., 1992. The measurement of sediment irrigation rates: a comparison of the Br-tracer and $^{222}Rn/^{226}Ra$ disequilibrium techniques. Journal of Marine Research 50, 125–154.

Meile, C., Karetsky, C.M., Van Cappellen, P., 2001. Quantifying bioirrigation in aquatic sediments: an inverse modeling approach. Limnology and Oceanography 46, 164–177.

Minoru, F., Murashige, S., Ohnishi, Y., Yuzawa, A., Miyaska, H., Suzuki, Y., Komiyama, H., 2002. Decomposition of phytoplankton in seawater. Part 1: kinetic analysis of the effect of organic matter concentration. Journal of Oceanography 58, 433–438.

Morse, J.W., Berner, R.A., 1995. What controls sedimentary C/S ratios? Geochimica et Cosmochimica Acta 59, 1073–1077.

Morse, J.W., Rowe, G.T., 1999. Benthic biogeochemistry beneath the Mississippi River plume. Estuaries 22, 206–214.

Rabalais, N.N., Wiseman Jr., W.J., Turner, R.E., 1994. Comparison of continuous records of near-bottom dissolved oxygen from the hypoxic zone along the Louisiana coast. Estuaries 17, 850–861.

Rabalais, N.N., Turner, R.E., Wiseman, W.J., 2002. Gulf of Mexico hypoxia, A.K.A. "the dead zone". Annual Review of Ecology and Systematics 33, 235–263.

Roden, E.E., Tuttle, J.H., 1992. Sulfide release from estuarine sediments underlying anoxic bottom water. Limnology and Oceanography 37, 725–738.

Rowe, G.T., Morse, J.W., Boland, G.S., Cruz-Kaegi, M.L., 1995. Sediment metabolism and heterotrophic biomass associated with the Mississippi River plume. Proceeding of the Synthesis Workshop on Nutrient Enhanced Coastal Ocean Productivity. NOAA, pp. 102–105.

Rowe, G.T., Cruz-Kaegi, M.L., Morse, J.W., Boland, G.S., 2002. Sediment community metabolism associated with continental shelf hypoxia, northern Gulf of Mexico. Estuaries 25, 1097–1106.

Sell, K.S., Morse, J.W., 2006. Dissolved Fe^{2+} and $\sum H_2S$ behavior in sediments seasonally overlain by hypoxic-to-anoxic waters as determined by ASV microelectrodes. Marine Chemistry 12, 179–198.

Van Cappellen, P., Wang, Y., 1996. Cycling of iron and manganese in surface sediments: a general theory for the coupled transport and reaction of carbon, oxygen, nitrogen, sulfur, iron and manganese. American Journal of Science 296, 197–243.

Zimmerman, A.R., Canuel, E.A., 2000. A geochemical record of eutrophication and anoxia in Chesapeake Bay sediments: anthropogenic influence on organic matter composition. Marine Chemistry 69, 117–137.